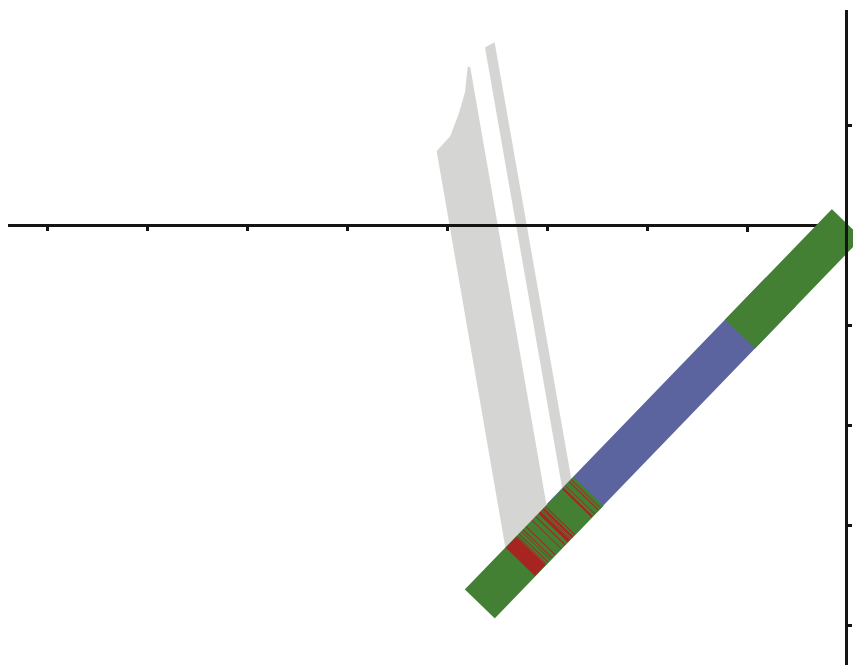


An anoxic, Fe(II)-rich, U-poor ocean 3.46 billion years ago

atmospheric O₂ levels prior to the GOE as compared to a simple “step-function” (Anbar et al., 2007; Kaufman et al., 2007; Wille et al., 2007; Garwin et al., 2009; Godfrey and Falkowski, 2009; Ono et al., 2009; Dan et al., 2010; Kendall et al., 2010; Voegelin et al., 2010; Caza et al., 2012; Reinhard et al., 2013).

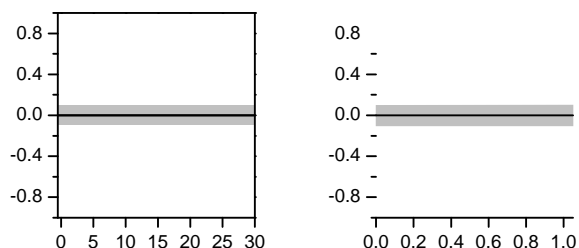
Attempts to constrain the evolution of oxygenic photosynthesis have been controversial. For example, the timing of the evolution of oxygenic photosynthesis has been partially constrained to ~2.7 Ga, based on molecular biomarkers (Brocks et al., 1999; Eigenbrode and Freeman, 2006; Eigenbrode et al., 2008; Waldbauer et al., 2009), although this line of research has been highly controversial (e.g. Rasmussen et al., 2008). Large microfossils of 3.4–3.1 Ga age have been interpreted to be possible eukaryotes or possible cyanobacteria, which, if confirmed, would suggest an even earlier origin for oxygenic photosynthesis (Sigitani et al., 2007, 2010; Janda et al., 2010). Other researchers point to geological evidence that may indicate still earlier oxygenation of the atmosphere, and therefore, a very early appearance of oxygenic photosynthesis. For example, hematite in the 3.46 billion-year-old (Ga) Marble Bar Chert Member (MBC), and in the stratigraphically younger Ape Basalt,



core for each hematite-bearing red layer of the MBC (Figs. 2 and 3). For U-Th-Pb isotope analysis, a larger slab (cm size, >0.15 g) was cut because of the very low U and Th concentrations in chert samples. Both hematite-rich red layers and hematite-poor white layers of the MBC were sampled. Samples were examined under a binocular microscope before and after cutting in order to ensure that

cracks, veins, and other secondary features were avoided. Samples were cleaned using acetone, 0.2 M HCl, and 18.2 MΩ H₂O in an ultrasonic bath for more than 10 min each to remove surface contamination, before being dried and weighed. This procedure ensured complete removal of any surface Fe, Pb and U contamination that may have been introduced during coring or sampling. Powder

samples of Ape Basalt and Deer Formation basalt that were analyzed for Fe isotope compositions were the same as those studied by [Li et al. \(2012\)](#), and sample preparation details may be found in that study.



trations in the basalts, nor between $\delta^{56}\text{Fe}$ anomalies and Fe/Th ratios (Fig. 4).

4.2.2. Lead concentrations

Lead concentrations in the MBC samples are between 0.37 and 12.95 ppm, U between 3 and 60 ppb, and Th between 4.5 and 42.23 ppb (Appendix 2). Concentrations of Pb, U, and Th are higher in the hematite-bearing red/black layers than in the hematite-poor, white layers (Figs. 2 and 3). Notably, concentrations of Pb, U, and Th in the MBC samples are systematically lower than those of the basaltic samples from the same drill core, which are 1.58 ppm for Pb, 80.1040 ppb for U, and 233.694 ppb for Th (Li et al., 2012). Importantly, U contents are much lower than those of modern oceanic sediments (0.306–4.889 ppm, global average 1.68 ppm; Plank and Langmuir, 1998). The MBC samples have non-radiogenic Pb isotope compositions (low $^{206}\text{Pb}/^{204}\text{Pb}$, $^{207}\text{Pb}/^{204}\text{Pb}$ and $^{208}\text{Pb}/^{204}\text{Pb}$ ratios relative to a chondritic standard) that, in general, overlap those of basaltic samples from the ABDP-1 drill core. The $^{206}\text{Pb}/^{204}\text{Pb}$ ratios of samples from a drill core depth of 169.6–169.8 m are between 13.699 and 13.891 (Fig. 2), which are systematically higher than the $^{206}\text{Pb}/^{204}\text{Pb}$ ratios of samples from a drill core depth of 176.90–170.00 m that are between 12.684 and 13.153 (Figs. 2 and 3).



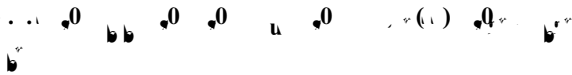
The hematite-bearing bands of the MBC have the highest $\delta^{56}\text{Fe}$ anomalies ever reported from natural black rocks (Fig. 5). These contrast sharply with the igneous and near-igneous anomalies (average $\delta^{56}\text{Fe} \sim 0\text{‰}$; Beard et al., 2003) of variably oxidized samples of the Ape Basalt (Fig. 4). The large contrast in Fe isotope compositions between hematite in the MBC and that in the oxidized portions (hematite and goethite; Kato et al., 2009) of the Ape Basalt indicates distinct processes of formation.

The small variation in $\delta^{56}\text{Fe}$ anomalies of the Ape Basalt (Fig. 4 and Table S1), averaging 0‰, suggests that Fe in Ape Basalt is primarily igneous in origin. The limited range in $\delta^{56}\text{Fe}$ anomalies, which occurs only in the most oxidized

samples, most likely reflects small extents of internal redistribution of Fe during oxidation. The fact that the two samples that have low $\delta^{56}\text{Fe}$ anomalies also have high Fe/Th ratios, and that the samples with the highest $\delta^{56}\text{Fe}$ anomalies also have low Fe/Th ratios (Fig. 4) implies that some samples might have released isotopically light Fe into fluids during weathering. This isotopically light Fe was then oxidized and re-precipitated, causing enrichment of isotopically light Fe oxides. Iron mobility could have been promoted by weathering of sulfides that were formed at 2.76 Ga at Marble Bar (Kato et al., 2009), which produced a locally acidic and redox-active environment that might enable small-scale Fe mobility and Fe isotope fractionation. Although Kato et al. (2009) suggest that oxidation occurred in the Archean, Li et al. (2012) documented Phanerozoic U mobility that correlated with the extent of oxidation,

indicating that oxidation of the Ape Basalt most likely occurred in a channelled ground water dredging deep Phanerozoic weathering. Under such conditions, large-scale Fe mobility would not be expected, and this is supported by the limited range in $\delta^{56}\text{Fe}$ values and the fact that the average $\delta^{56}\text{Fe}$ value lies at the value for igneous rocks.

In the MBC, the very high $\delta^{56}\text{Fe}$ values rule out the possibility that Fe was transported from the Ape Basalt. Moreover, the very high $\delta^{56}\text{Fe}$ values of the MBC are inconsistent with hematite formation by in situ oxidation of Fe(II)-bearing minerals such as siderite, as has been proposed for some jaspers in the underlying Dresser Formation (Van Kranendonk et al., 2008). Siderite that precipitated from an Archean ocean should have had a $\delta^{56}\text{Fe}$ value below -0.5‰ (Polak and Mineev, 2000; Wiesli et al., 2004; Johnson et al., 2008; Rastad et al., 2010), and in situ alteration to hematite should retain the negative $\delta^{56}\text{Fe}$ values. Furthermore, the low solubility of Fe(III) oxides and hydroxides at circumneutral pH (e.g., Kuma et al., 1996, and references therein) makes it unlikely that significant quantities of Fe could be leached from the MBC under oxidized conditions. We therefore conclude that the hematite in the MBC was not produced by the Phanerozoic oxidation event that oxidized the Ape Basalt at Marble Bar. This interpretation is consistent with the fracture and vein patterns in the drill core (Fig. 1C), that suggest ground water movement was likely along channelled fracture systems.



The likely source of aqueous Fe(II) that was oxidized to form hematite in the MBC is hydrothermal fluids, which should have had a $\delta^{56}\text{Fe}$ value of around 0‰ , or slightly negative (Yamaguchi et al., 2005; Johnson et al., 2008). Oxidation of aqueous Fe(II) in modern marine hydrothermal systems produces precipitates that have slightly negative $\delta^{56}\text{Fe}$ values (Fig. 5), reflecting essential quantities of oxidation. The very high $\delta^{56}\text{Fe}$ values of hematite in the MBC, therefore, do not support a full oxidized Archean ocean, as proposed by Hoashi et al. (2009). Rather, the very high $\delta^{56}\text{Fe}$ values can only be explained by partial oxidation of aqueous Fe(II), given the $\sim 3\text{--}4\text{‰}$ fractionation in $^{56}\text{Fe}/^{54}\text{Fe}$ between oxides and aqueous Fe(II) (Wright et al., 2012).

Constraints on the extent of oxidation of aqueous Fe(II) in an Archean ocean can be made using a one-dimensional dispersion/reaction model, which assumes aqueous Fe(II) released from hydrothermal vents disperses upwards to the photic zone, followed by oxidation of Fe(II)_{aq} to Fe(III) hydroxides (Cajava et al., 2012, 2013). The limitation of the dispersion/reaction model is that it may not accurately describe pilling of hydrothermal Fe(II), as the solution of the model relies on a steady-state condition of the ocean. Nevertheless, the dispersion/reaction model is superior compared with a simple Rayleigh fractionation model that is commonly used in geochemical studies, which is not an appropriate model for interpreting Fe isotope fractionation during oxidation in the photic zone because it is a closed-system model and does not account for a continual in

of Fe(II)_{aq} and outflow of Fe(OH)₃ precipitates. Using the dispersion/reaction model of Cajava et al. (2012, 2013), we produced vertical profiles for concentrations and isotope compositions of Fe(II)_{aq} and Fe(OH)₃, at different rates of Fe(II)_{aq} oxidation (Appendix 3). In the model, oxidation could occur either anaerobically or aerobically, which simulates oxidation by either anoxygenic Fe(II)-oxidizing photosynthetic bacteria, or by free oxygen generated by oxygenic photosynthetic bacteria, respectively; in the latter case, our model can provide constraints on the amount of free oxygen that may have been present.

The dispersion/reaction model of Cajava et al. (2012, 2013) produces broadly similar profiles of concentrations and isotopic compositions of Fe(II)_{aq} and Fe(OH)₃ over a

estimated for the photic zone are less than 10^{-3} μM to produce the high measured $\delta^{56}\text{Fe}$ values, which is less than 0.0003% of modern O_2 contents in the photic zone. This conclusion is robust and is insensitive to changes in input parameters, including choice of $\text{Fe}(\text{OH})_3/\text{Fe}(\text{II})_{\text{aq}}$ Fe isotope fractionation factors, although the latter parameter would be important if attempting to distinguish between O_2

bounds calculated here, given that [Li et al. \(2012\)](#) documented increases of up to 890% in the U/Th ratios of the ABDP-1 basalts during the Phanerozoic.

Uranium contents of seawater may be constrained using the U_{adsorbed} calculated above, the iron oxide contents of the MBC, and data on U adsorption coefficients measured for iron oxides/hydroxides. Adsorption coefficients for U are generally high for Fe(III) oxides and hydroxides, more than

diating bacteria, or free oxygen produced by oxygenic photosynthesis. Although UV photo-oxidation of $\text{Fe(II)}_{\text{aq}}$ has been proposed as a mechanism for Fe(III) oxide precipitation in the Archean (Braterman et al., 1983), this is not supported by the experimental work of Konhauser et al. (2007), which demonstrated that UV photo-oxidation oc-

shale (*Gastrioceras listeri* Marine Band) and associated strata;
England. *Chem. Geol.* , 605-621.

Van Kranendonk M. J., Hickman A. H., Smithies R. H., Nelson D. R. and Pike G. (2002) Geology and tectonic evolution of the Archean North Pilbara Terrain, Pilbara Craton, Western Australia. *Econ. Geol.* 5, 695-732.